







# Analysis and Modeling of Pedestrian Flow in a Confined Corridor Focusing on the Headway Distance and Velocity of Pedestrians

Yoshikazu Minegishi <sup>\*</sup>, Takenaka Corporation, 1-1-1 Shinsuna, Koto, Tokyo 136-0075, Japan

Yoshifumi Ohmiya , Tokyo University of Science, 2641 Yamazaki, Noda, Chiba 278-8510, Japan

Tomonori Sano , Waseda University, Mikajima 2-579-15, Tokorozawa, Saitama 359-1192, Japan

Manabu Tange , Shibaura Institute of Technology, 3-7-5 Toyosu, Koto, Tokyo 135-8548, Japan

**Received:** 18 January 2021/**Accepted:** 25 August 2021/**Published online:** 8 September 2021

**Abstract.** In fire evacuation situations, at corridors, many evacuees are plagued by high density, low velocity, and long waiting time. Therefore, engineers have to consider the countermeasure preventing crowd accidents. For this purpose, the development of pedestrian simulators that are constructed with concrete physical parameters, such as the headway distance between pedestrians, velocity, and specific flow, is required. To acquire the evacuation behavior in corridors, we conducted well-controlled pedestrian walking experiments in a confined corridor with realistic architectural geometry and modeled the pedestrian behaviors. An experimental loop corridor was constructed to acquire stable pedestrian flows without distractions from bottlenecks or merging flows. We conducted five experiments with different density patterns with an average density ranging from 1.28 to 3.42 people/m<sup>2</sup> and a maximum of 96 test participants. We found that when the headway distance is 0.55–1.15 m, the velocity increases linearly with increasing headway distance, similar to single-file experiments. When the density is higher than 2.35 people/m<sup>2</sup>, the pedestrians cannot walk at a constant speed, and they exhibit stop-and-go behavior. In this situation, the percentage of pedestrians who walk at a headway distance of approximately 0.4–0.5 m, which is the minimum headway distance, increases. In addition, the fundamental diagram between density and velocity is acquired at a density higher than 1.4 people/m<sup>2</sup> as an inversely proportional function. The density dependence on the specific flow is a linear function. The maximum specific flow is acquired at the marginal minimum density where a linear relationship is maintained.

**Keywords:** Evacuation, Pedestrian, Headway distance, Density, Velocity, Specific flow

<sup>\*</sup>Correspondence should be addressed to: Yoshikazu Minegishi, E-mail: Minegishi.yoshikazu@takenaka.co.jp



## 1. Introduction

Considering the evacuation of many people from rooms that are on fire, such as theatres, conference rooms, and offices, the evacuation flow is restricted by bottlenecks such as doors (Fig. 1, a1). Many researchers have studied bottleneck flows [1–11] (Fig. 1, a2), and specific flows and densities in front of these bottlenecks were examined. In bottleneck flows, the density can differ whether in front of the bottleneck, passing through the bottleneck or having cleared the bottleneck. Moreover, the density is affected by the rate of arrival of evacuees to the bottlenecks, and the arrival rate is also time-dependent [1, 2, 4, 6, 9–11]. Another phase of fire evacuation safety is the evacuation behavior in corridors or the circulation spaces connected to fire rooms, stairs or the outside. This should also be considered carefully. Usually, these spaces are relatively safe from fire and smoke (Fig. 1, b1.) However, many evacuees are expected to accumulate at a high density and may endure long waiting time at low velocity (Fig. 1, b2.) Therefore, we examine stable and high-density crowd flows within a confined corridor with the goal of contributing to engineering design to prevent crowd accidents.

Usually, crowd flow is represented by a fundamental diagram that represents the relationship between the average density, velocity, and specific flow, and many regression models using these values have been proposed through experiments and on-site observations [12–20]. One of the most famous references for actual fire evacuation design is SFPE's fundamental diagram [16], which is derived from macroscopic observations of pedestrian walking behaviors [21, 22]. This diagram models the relationship between the pedestrian density and specific flow through a quadratic function, and this simple modeling is beneficial for engineering design, especially in early design stages.

The concept of a fundamental diagram implicitly assumes that density and velocity are uniquely correlated with each other; however, the strength of this correlation has not been examined. Moreover, based on this concept, all pedestrians in a crowd walk at the same low velocity; thus, the crowd flow becomes homogeneous and steady. However, the application limit of this concept has not been clarified. In addition, many researchers have analyzed bottleneck flows by focusing on the density in front of a bottleneck and the specific flow through it [1, 2, 4, 6, 9, 11], and sometimes these are discussed in terms of fundamental diagrams [1, 2, 9, 11]. However, we consider the difference between bottleneck flows and corridor flows in the generating mechanism of the crowd. In bottleneck flows, the density can differ whether in front of the bottleneck, passing through the bottleneck or having cleared the bottleneck. Moreover, the density is affected by the arrival rate of evacuees, and the bottleneck arrival rate is also time-dependent (Fig. 1, a2.) On the other hand, corridor flows are relatively stable. Therefore, it is not necessarily self-evident that these are the same phenomena, and they should be considered separately. Therefore, we also examine crowd behavior and the applicability limit of the fundamental diagram for corridor flows.

In contrast, current multiagent pedestrian simulators model individual pedestrian walking behavior, and crowd flows are represented by the emergence of

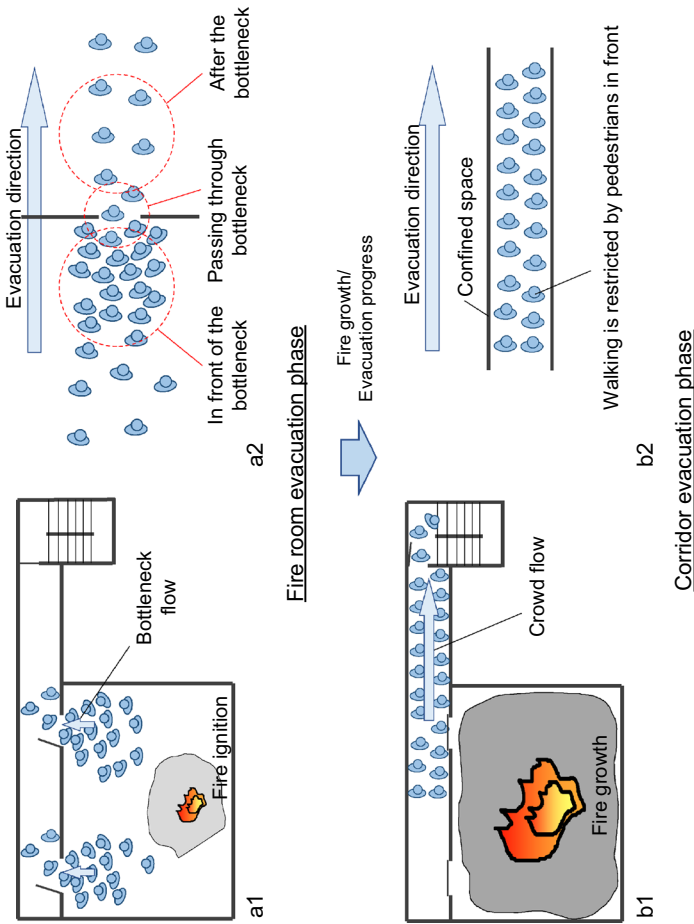


**Figure 1. Fire room evacuations and corridor evacuation/bottleneck flows and corridor flows.**

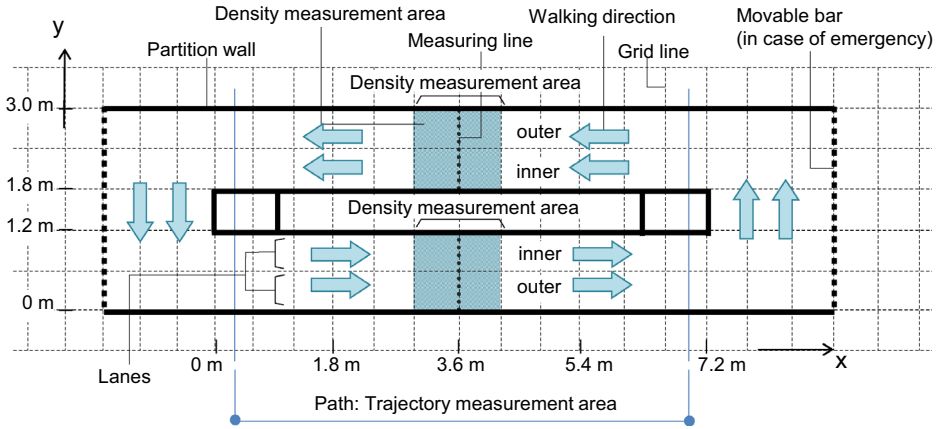


**Figure 2. Layout of the experimental corridor.**

interactions among pedestrians. In this sense, the density itself is one of the outcomes. Modeling individual pedestrian walking behavior by more concrete physical parameters, such as the distance between pedestrians in the walking direction (referred to as the headway distance) [23–26], is required to construct a more reliable and expandable pedestrian simulator. For example, in practical evacuation safety design, controlling accumulation and its density is one of the most critical issues [27]. To precisely simulate this behavior, the behavior of individual pedestrians has to be adequately modeled.

As the simplest and most fundamental crowd walking behavior, the so-called single-file pedestrian flow, has been intensely studied [24, 28–36]. This approach can represent a crowd through the expansion of the emergence of aggregation from the microscopic behaviors of individuals. Moreover, this kind of research is rapidly being promoted by the digital image processing of pedestrian motion [37–40]. However, many previous single-file experiments did not reproduce realistic architectural geometry or crowd walking. Some constructed a loop path by pipe chairs with a waist height that did not constrain arm and shoulder movements [24, 35, 36]. Some constructed their paths as 0.8 m wide [24, 31, 33, 35]; however, considering the actual architectural geometry, the minimum width of an evacuation route is 1.12 m according to the NFPA Life Safety Code [41] or 1.2 m according to the Building Standard Law in Japan [42], and in those corridors, evacuees can walk in two lanes. Even though we analyze the crowd flow focusing on the headway distance to the forward pedestrian, it is desirable to reproduce the walking environment realistically.

Considering the current demand for evacuation simulators and the progression of measurement and analysis technology, we tried to determine the characteristics of stable crowds with well-controlled pedestrian walking experiments and analyze crowd and individual pedestrian behaviors. We focused on not only macroscopic aspects, such as the average velocity, density, and specific flow, but also microscopic aspects, especially the relationship between the headway distance and veloc-

ity. Through these experiments and analyses, we propose a better fundamental diagram that is fit for multiagent pedestrian simulators and fire safety design.

## 2. Methodology

### 2.1. Stable Crowd Flow and Loop Corridor Experiments

To understand and model the fundamental behavior of a crowd, stable crowd flows during evacuation are reproduced. In this research, we define “stable” as a flow being homogeneous and steady over the whole range of the flow, or there being some periodic unevenness of density. Thus, a specific flow is either constant or periodic. This means that the density does not keep increasing or decreasing, such as at bottlenecks or merges. The concept of fundamental diagrams [12–20] explicitly expects that the relationship between density and velocity or density and specific flow has a one-to-one correspondence. We initially examine this hypothesis by checking that the flow converges homogeneously and steadily. We also determine whether this hypothesis can be applied for crowds with periodic unevenness.

To create such a stable crowd, we developed the experimental loop corridor depicted in Fig. 1. The supposition for this setting is that by keeping the pedestrians walking in the loop corridor, they adjust their velocity and distance from the surrounding pedestrians and walls. We expected that their walking status would gradually converge.

### 2.2. Settings of the Experimental Loop Corridor

The experimental loop corridor is depicted in Fig. 2, 3 and 4; it is 7.2 m long (defined as the x-direction) and 1.2 m wide on the longer side and 3.0 m long (defined as the y-direction) and 1.8 m wide on the shorter side. The objective of this experiment is to obtain a stable flow along a straight corridor. Hence, the shorter side is wider than the longer side to avoid impeding the pedestrian flow when changing direction at the corner. The outer and inner walls are made of 1.8 m high partitions. Both short sides are partitioned by plastic bars at the height of

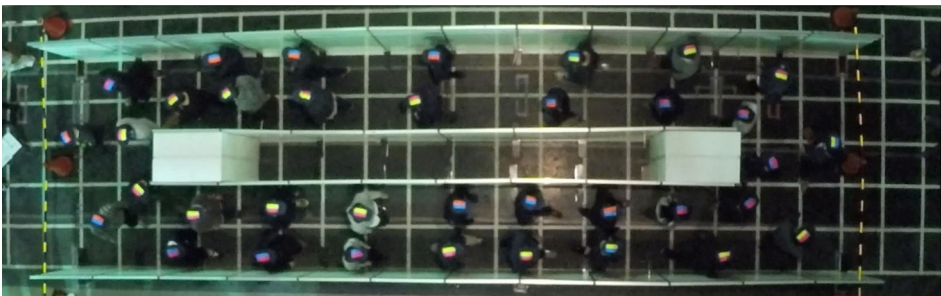


**Figure 3. Picture of the experimental corridor and the allocation of occupants [Case 1: 36 people].**

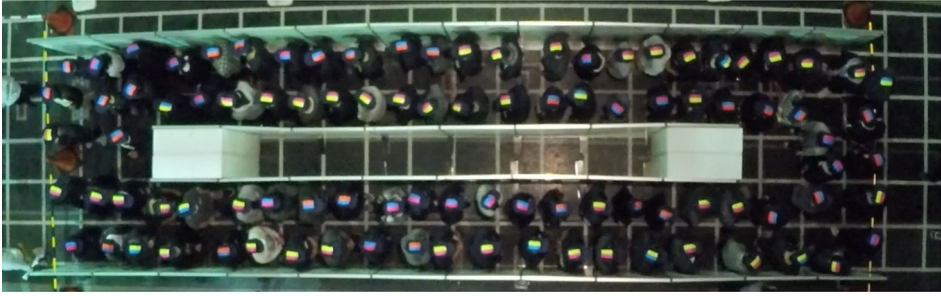


**Figure 4. Picture of the experimental corridor and the allocation of occupants [Case 5: 96 people].**

**Table 1  
Experimental Case Settings**

Case no	Number of pedestrians [people]	Target average density [people/m <sup>2</sup> ]	Actual average density [people/m <sup>2</sup> ]
Case 1	36	1.28	1.42–1.50
Case 2	48	1.71	1.73–1.89
Case 3	66	2.35	2.47–2.72
Case 4	78	2.78	2.58–3.04
Case 5	96	3.42	2.90–3.68

Target average density: number of pedestrians divided by the total area of the experimental corridor

Actual average density: total time-average density at the 1.2 m range of the center of the experimental corridor

the pedestrian's waist. Grids of 600 mm × 600 mm are lined with white tape for imaging analysis, and pedestrians are evenly arranged in initial positions.

### 2.3. Experimental Conditions

The experiments were conducted in the laboratory building of the Tokyo University of Science on October 24, 2015. On this day, six types of crowd flow experiments were conducted, and this loop corridor experiment was the first experiment among them.

The five average density conditions presented in Table 1 were set by changing the number of pedestrians in the experimental corridor. A total of 96 test participants (62 males and 34 females, aged 20 to 25, including university students, graduate university students, and vocational school students) were divided into eight groups of 12 pedestrians. The pedestrians were almost homogeneous demographically and consisted of able-bodied adults who were not excessively obese or elderly. An actual population is diverse regarding age, gender, body size, walking speed, cultural background, and level of mobility. Thus, these differences and mixtures should be considered for a fire evacuation design. Some research has considered mixtures of elderly [43, 44] or slower pedestrians [45]. However, if the experiments are conducted with such a diverse group of people, it becomes too

difficult to analyze the mechanism of the crowd flow to distinguish how and to what extent a certain factor affects the crowd flow. Therefore, we only recruited nearly homogeneous and healthy people as test participants.

The five average density conditions listed in Table 1 were set by using a combination of those groups. All experiments were conducted two times.

#### **2.4. Experimental Procedure**

For the initial condition, the pedestrians were allocated to an almost uniform density in the loop corridor. After that, they were directed by an experimenter to walk in a counterclockwise direction. They walked for more than 70 s, and they stopped walking at the instruction of an experimenter. The time interval of 70 s was decided through test experiments to acquire a stable state. For example, in Case 1 and Case 2, pedestrian velocity was slow for a few seconds after the onset of walking; however, their velocity became almost constant (this can be identified in the figures shown later in Sect. 4.2.). Because the corridor was a loop, they could walk continuously. Therefore, a stable crowd flow was expected to develop. Five seconds before starting to walk, the pedestrians were directed to step on a particular spot, and after that, they started walking at the cue of “Start walking.” In addition, every pedestrian performed a practice walk for 1 min before the actual experiments. Subsequently, the actual experiments were conducted from Case 1 to Case 5. After Case 5 was finished, Cases 1 to 5 were conducted again; hence, each case was conducted twice.

The pedestrians were instructed to assume that they were in a fire situation and to walk swiftly but not run or push other test participants. One of the intentions of this instruction is for the safety of the test participants, that is, to become test participants in an excessively rushed situation. Another purpose is that this research is focused on “corridor flow”, which means that it is not focused on “bottleneck flow.” For example, if a fire occurs in a room, such as an office room, atrium, theater, etc., occupants in the room need to evacuate quickly to avoid direct smoke exposure. After they reach a relatively safe area or circulation space, such as a corridor, foyer, or concourse, evacuees are relieved compared with the situation in which they were in the room. In this evacuation phase, the main concern is to avoid crowd accidents, such as excessive heavy congestion and high density situations. Even though we instructed test participants to imagine a fire evacuation situation, it is expected that they would not necessarily hurry as in a real fire situation, and they did not consider the situation to be a fire evacuation or corridor evacuation. However, considering the focused situation and with some conservative consideration, the modeling of crowd flow based on this experiment contributes to the design of a safe and effective circulation space design.

#### **2.5. Measurements**

We employed Tange’s measurement methodology [40]. A video camera was installed approximately 10 m above the experimental loop corridor, and the walking behavior was recorded. We recorded the videos at a frame rate of 1/30 s; hence, the x- and y-coordinates were obtained every 1/30 s. To precisely and clearly



obtain the pedestrian positions, we provided caps with two colors of matte tapes to all the pedestrians. After the experiments, through the tracking of these colors on the videos, every pedestrian's coordinates and trajectories were determined. The images were distorted depending on the distance from the center of the image. The x- and y-coordinates of the image were different from the actual pedestrian positions because of the difference in each pedestrian's height. Therefore, the x- and y-coordinates were determined using geometrical correction of the distortion and differential.

### 3. Analysis Method

We conducted two kinds of analyses: microscopic analysis and macroscopic analysis. We analyzed the time-historical position, headway distance and velocity of individual pedestrians via microscopic analysis. In the macroscopic analysis, we examined the relationships between the density, velocity, and specific flow. In this analysis, we focused on the range of 1.2 m at the center of the loop corridor in Fig. 2.

#### 3.1. Microscopic Analysis

*3.1.1. Headway Distance* In previous studies [12–20], the fundamental diagram of crowd flow is expressed as a relationship between the density and velocity or density and specific flow. This concept assumes that pedestrian walking behavior is affected or determined by the density. In our supposition, the headway distance is thought to be the dominant effect on density. In addition, in this experiment, pedestrians walked in almost two lines. As such, we analyzed the experimental data in terms of the headway distance. Although no instruction to form two lines in the path was given to the pedestrians, they walked in almost two lanes. Therefore, we measured the headway distance  $d$  (m). Headway distance is defined as the distance between the heads (center of the two color tapes on the test participants' caps) of consecutive pedestrians. The distance in the y-direction (lateral distance) is not considered for headway distance (Fig. 5.)

*3.1.2. Velocity* The velocity  $v$  (m/s) at time  $t$  (s) was calculated as the walking distance within  $7/30$  s (from time  $t - 3/30$  s to  $t + 3/30$  s) divided by  $7/30$  s. To acquire the relationship between velocity and headway distance or velocity and density, the time interval should be small to some extent. If the time interval is large, the plot dispersion of headway distance to velocity is small because the impact of the error becomes relatively small. On the other hand, if the time interval is too small, walking sway strongly affects the measured velocity, especially in a slow velocity situation. With this  $7/30$  s time interval, some negative velocity caused by longitudinal sway (x-direction) in an almost stopped situation is observed. The average of those negative velocities in Case 5, the densest and lowest velocity case, is approximately  $-0.026$  m/s, and less than 2% of the negative velocity data are smaller than  $-0.1$  m/s. Considering that the measurement error stems from the image processing data acquisition, this negative velocity is regar-



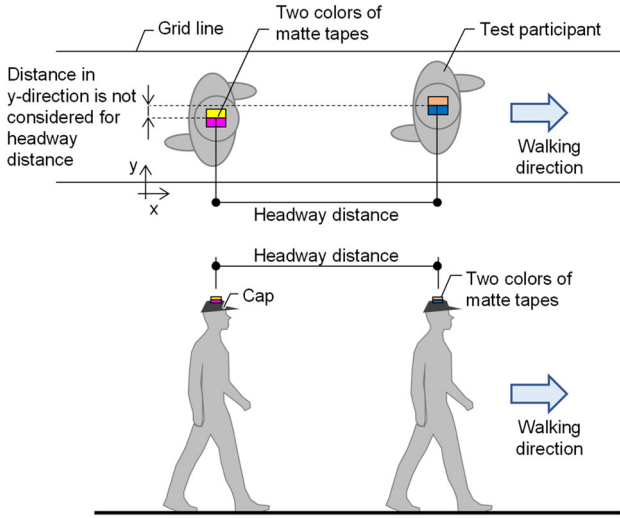


**Figure 5. Definition of the headway distance.**

ded within the error. Walking sway can affect the y-direction (lateral direction). The average of those negative velocities in Case 5 is approximately  $-0.074$  m/s, and less than 7.2% of the negative velocity data are smaller than  $-0.2$  m/s. However, the velocity in the y-direction is not used in this research.

*3.1.3. Two-Dimensional Histogram of v-d* We acquired the relation between  $d$  and  $v$  of all pedestrians in every position frame in a two-dimensional histogram. This histogram was acquired as follows: The data points of  $d$  and  $v$  of all pedestrians in the range of  $x = 0$  m to  $x = 7.2$  m in each lane (each corridor had two lanes, the inside and outside) of each corridor ( $y = 0$  m to 1.2 m and  $y = 1.6$  m to 2.8 m) were acquired per  $1/30$  s for approximately 70 s. Just accumulating every data point was simple. However, the numbers of data points from the experimental cases differ. Considering these differences, we normalized the data distribution by experimental cases  $c$  (–) (five experimental cases; see Table 1), lanes  $l$  (–) (we had four lanes,  $y = 0$  m to 0.6 m,  $y = 0.6$  m to 1.2 m,  $y = 1.8$  m to 2.4 m, and  $y = 2.4$  m to 3.0 m; see Fig. 2), and number of trials of experiment  $k$  (–) (we performed two trials of each experimental case). In the analysis of each experimental case, we normalized to intervals of 0.01 m/s for  $v$  and 0.01 m for  $d$  as follows:

$$N(v, d)_c = \frac{\sum_l \sum_k P_{v,d,c}(l, k)}{\sum_l \sum_k P_{all,c}(l, k)} \tag{1}$$

$$Q_c = \sum_v \sum_d N(v, d)_c = 1 \tag{2}$$

$N(v, d)_c$ : Normalized value for the specific intervals of  $v$  and  $d$  in experimental case  $c$  (-).

$P_{v,d,c}(l, k)$ : Number of data points for the specific intervals of  $v$  and  $d$  in case  $c$ , lane  $l$ , and trial number  $k$  (points)\*\*

$P_{all,c}(l, k)$ : Number of data points for all pedestrians (all intervals of  $v$  and  $d$ ) in case  $c$ , lane  $l$ , and trial number  $k$  (points).

$Q_c$ : Sum of the normalized values of all intervals of  $v$  and  $d$  in the experimental case  $c$  (-).

In the analysis of the consolidated experimental cases, we normalized to intervals of 0.1 m/s in  $v$  and 0.1 m in  $d$  as follows:

$$N(v, d, c, l, k) = \frac{P_{v,d,c,l,k}}{P_{all,c,l,k}} \quad (3)$$

$$\begin{aligned} Q &= \sum_v \sum_d \sum_c \sum_l \sum_k N(v, d, c, l, k) \\ &= 1 \times 5 \times 4 \times 2 = 40 \end{aligned} \quad (4)$$

$N(v, d, c, l, k)$ : Normalized value for the specific intervals of  $v$  and  $d$  in experimental case  $c$ , lane  $l$ , and trial number  $k$  (-).

$P_{v,d,c,l,k}$ : Number of data points for the specific intervals of  $v$  and  $d$  in case  $c$ , lane  $l$ , and trial number  $k$  (points).

$P_{all,c,l,k}$ : Number of data points for all pedestrians (all intervals of  $v$  and  $d$ ) in case  $c$ , lane  $l$ , and trial number  $k$  (points).

$Q$ : Sum of the normalized values of all intervals of  $v$  and  $d$  in all  $c$ ,  $l$ , and  $k$  (-).

### 3.2. Macroscopic Analysis

Basically, the pedestrians formed two lines in almost all cases and at all times. In this sense, these pedestrians approximated one-dimensional flow, in which the relationship between pedestrians is represented by the one-dimensional headway distance, i.e., not by the density. However, to understand this characteristic more thoroughly, we compared the preceding research and fundamental diagrams. We analyzed the experimental data focusing on the density in an area sized 1.2 m  $\times$  1.2 m at the center of the loop corridor (explained in Sect. 4: Analysis method).

**3.2.1. Density** We focused on the time  $t$  at which each pedestrian passed through the line of  $x = 3.6$  m (Fig. 2). The number of pedestrians in the section of 1.2 m from  $x = 3.0$  m to 4.2 m was counted at each selected time  $t$ , and the density  $\rho$  (people/m<sup>2</sup>) at the section of length 1.2 m by width 1.2 m was calculated. We regarded this density as the surrounding density of the pedestrian who passed  $x = 3.6$  m at time  $t$ .

This procedure to determine time  $t$  is applied for all experimental cases, that is, low-density cases to high-density cases. In the low-density case, the density and

velocity are almost homogeneous throughout the corridor. However, in the high-density case, the crowd flow became stop-and-go behavior [28], which is presented in the following chapter. This means that a large part of the crowd flow is almost stopped and some small part that is relatively low density is the only one walking. Therefore, with the above procedure, the density of only the relatively low-density part is measured. This aspect is common to the velocity explained next.

**3.2.2. Velocity** We focused on the time  $t$  at which each pedestrian passed through the line of  $x = 3.6$  m (see Fig. 2). For every pedestrian who passed through  $x = 3.6$  m within  $t - 0.5$  to  $t + 0.5$ , the moving distance was obtained by subtracting the  $x$ -coordinate value at  $t - 0.5$  from that at  $t + 0.5$ . This distance was regarded as the velocity at  $x = 3.6$  m and time  $t$ . The  $y$ -coordinate of every pedestrian also changed to some extent, but only the  $x$ -coordinate change was considered to determine the velocity of the  $x$ -direction component. Therefore, this velocity was specific for the pedestrian who passed  $x = 3.6$  m at time  $t$ .

This procedure to determine time  $t$  is applied to all experimental cases, that is, low-density cases to high-density cases. In the low-density case, the density and velocity are almost homogeneous throughout the corridor. However, in the high-density case, the crowd flow became stop-and-go behavior [28], which is presented in the following chapter. This means that a large part of the crowd flow is at slow velocity or almost stopped, and a small part that is at relatively low density is only walking. Therefore, with the above procedure, the density of only the relatively low-density part is measured. This aspect is common to the specific flow explained next.

**3.2.3. Specific Flow** The specific flow  $N$  (people/m/s) at  $x = 3.6$  m was measured. To obtain the specific flow at  $t$ , when a pedestrian passed through the line at  $x = 3.6$  m, the number of pedestrians who passed through  $x = 3.6$  m within 3 s from  $t - 1.5$  to  $t + 1.5$  was measured. Finally, the specific flow was calculated by dividing the number by the corridor width, 1.2 m. We regarded this specific flow as specific to the pedestrian who passed  $x = 3.6$  m at time  $t$ .

## 4. Results and Discussion

### 4.1. Overall Walking Behavior

Although no instruction was given to the pedestrians to form two lanes in the corridor, they walked in almost two lines. In addition, the velocities obtained in this experiment were slightly slower than those in subsequent experiments conducted on the same day, on bottleneck passing, straight corridors, and merging flows.

In Case 1 and Case 2, all pedestrians walked at almost the same velocity during walking. In Case 3, most of the pedestrians exhibited velocities lower than those in Case 1 and Case 2. However, some pedestrians in some parts of the corridor walked at high velocities, similar to Case 1 and Case 2. This fast velocity area looks like a longitudinal wave proceeding opposite to the pedestrians' walking direction (Fig. 6.) In Case 4 and Case 5, most pedestrians almost stopped, and

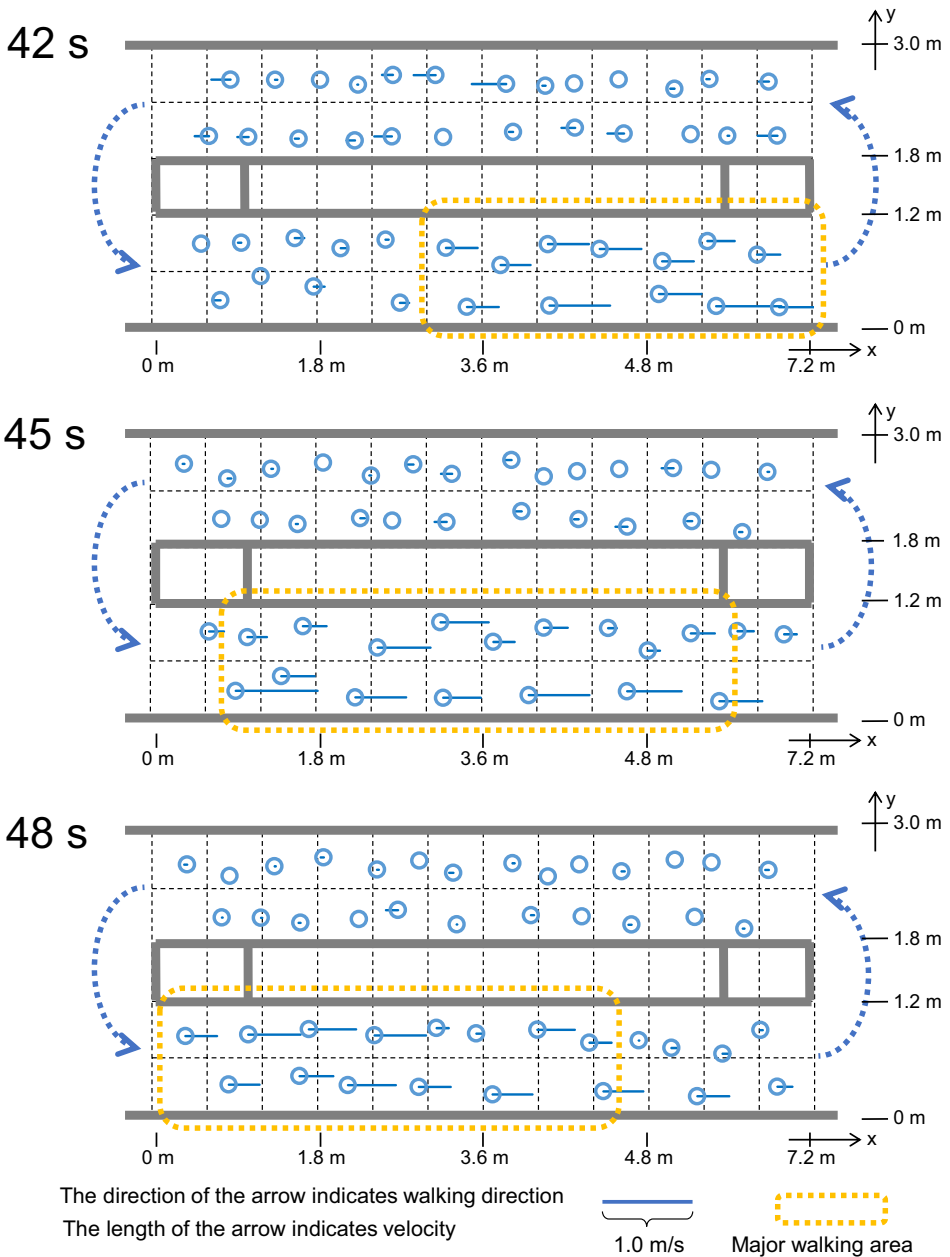


**Figure 6. Example of longitudinal waves proceeding opposite to pedestrians' walking directions (Case 4).**

some pedestrians along some of the corridor walked at low velocities. This behavior was similar to stop-and-go behavior [28].

We discuss the effect of the design of the experimental corridor in which the shorter side is wider than the longer side. From the video observation, in the low-density cases of Case 1 and Case 2, there is little difference in the flow status at the longer side and shorter side, or the velocity of the outer side of the shorter side is slightly larger. However, this velocity difference has little effect on the overall pedestrian flow. Additionally, from the video observation, in the high-density cases of Case 3, Case 4, and Case 5, some part of the longer side of the pedestrians almost stopped. Suppose the longer side of pedestrians stopped, following pedestrians at the shorter side are impeded by the pedestrian in front. When the longer side of pedestrians becomes low density and start to walk, the following pedestrians also begin to walk. The origin of the low-density area was the slight unevenness of the initial distribution of pedestrians. In some cases, the shorter side was the origin of the low-density area; however, there were also cases in which the longer side was the origin of the low-density region. Therefore, we considered that the stop-and-go behavior was not caused by the broader width of the shorter side, but it was generated by the slight unevenness of the initial distribution of pedestrians.

## 4.2. Microscopic Analysis

*4.2.1. Time–Space Diagram* Figures 7, 8, 9, 10 and 11 (left) show time–space diagrams of the pedestrians. In the graph, the  $x$ -axis denotes time, and the  $y$ -axis denotes the  $x$ -coordinate of the loop corridor. Hence, the trajectories in the graph show the time history of the  $x$ -coordinate of each pedestrian. The trajectories of the two pedestrians in all cases were similar. This result means that two pedestrians from the inner and outer sides walked abreast for most of the straight corridor, even though we did not instruct the participants to do so. The trajectories in Case 1 and Case 2 were almost parallel. This result implies that every pedestrian kept walking at almost the same velocity.

The trajectories in Case 3 to Case 5 consisted of high-gradient and low-gradient or almost horizontal sections. In the high-gradient sections, the pedestrians walked at relatively high velocities, and in the low-gradient or horizontal sections, the pedestrians walked slowly or even stopped. In the high-density cases of Case 4 and Case 5, not all pedestrians could walk, and stop-and-go behaviors were generated. In Cases 3 to 5, the time section where the trajectories steeply rose to the upper right is shown as bands stretching to the upper left. This behavior means that the high-gradient sections moved backward, similar to longitudinal waves. A pedestrian in a low-density section walks at high velocity, and the distance between the person and the following person increases; then, the following person can walk at a high velocity. In this sense, in a high-density crowd, the crowd flow is formed by a partial walking sequence, not by the homogeneous and steady walking of all the pedestrians. From the video observation, stop-and-go behavior originated from the slight unevenness of the initial distribution of pedestrians, and it originated not only from a shorter corridor but also from a longer corridor. If

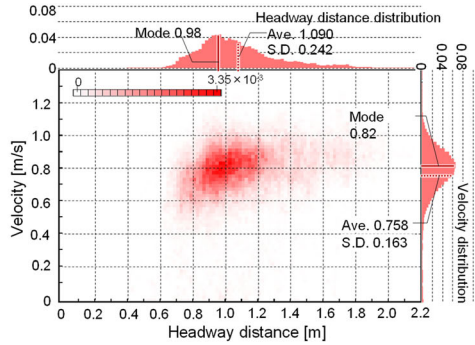
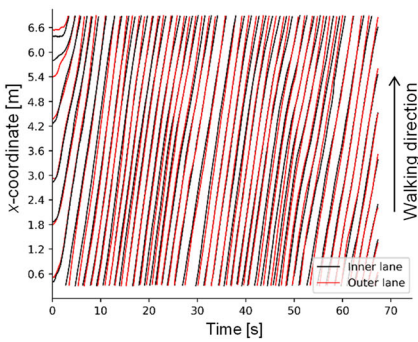


**Figure 7. Occupant trajectory (left) and normalized headway distance-velocity distribution (right) [Case 1: 1.28 persons/m<sup>2</sup>].**

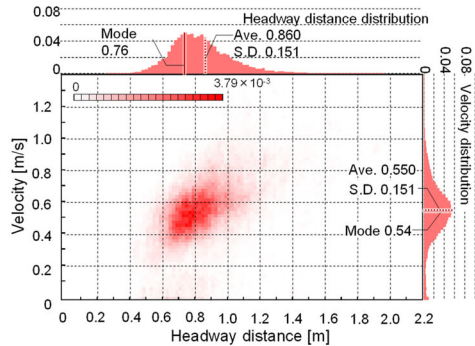
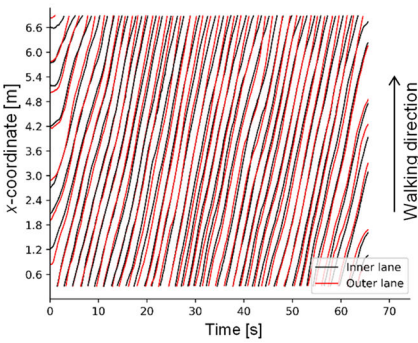


**Figure 8. Occupant trajectory (left) and normalized headway distance-velocity distribution (right) [Case 2: 1.71 persons/m<sup>2</sup>].**

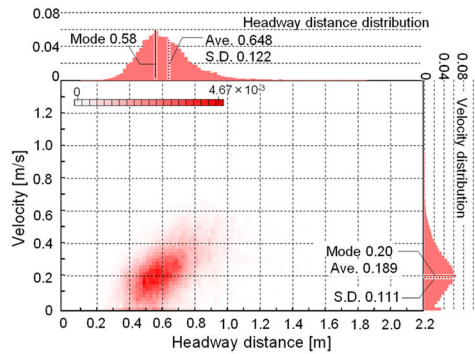
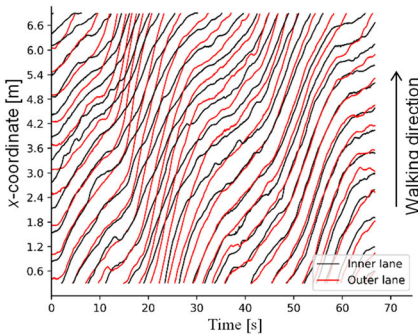


**Figure 9. Occupant trajectory (left) and normalized headway distance-velocity distribution (right) [Case 3: 2.35 persons/m<sup>2</sup>].**



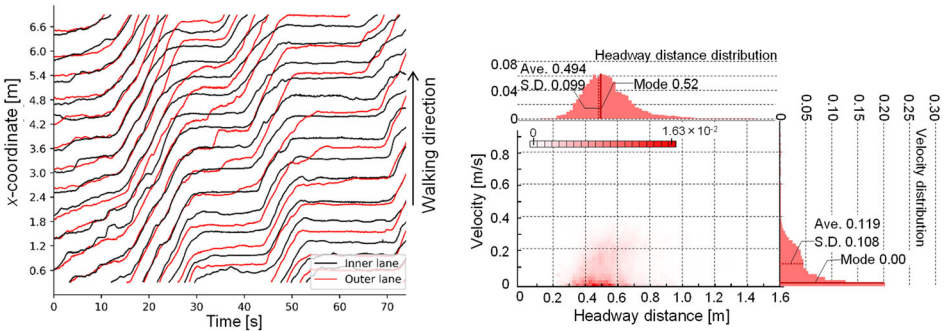


**Figure 10. Occupant trajectory (left) and normalized headway distance-velocity distribution (right) [Case 4: 2.78 persons/m<sup>2</sup>].**

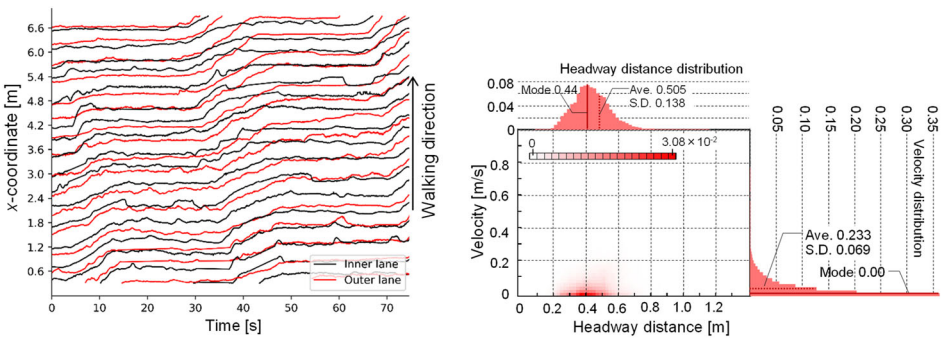


**Figure 11. Occupant trajectory (left) and normalized headway distance-velocity distribution (right) [Case 5: 3.42 persons/m<sup>2</sup>].**

the shorter corridors have a high velocity, the velocity at the end of the longer corridors, such as  $x = 6.6$  m, is always large. However, the velocity at  $x = 6.6$  m is not always high, and the high-velocity section moves backward. Therefore, the effect of the shorter side is not the only reason to generate unevenness of crowd flow.

In Case 3, there were steep-gradient trajectories (high velocity) and low-gradient trajectories (low velocity) for abreast pedestrians from 20 to 30 s, especially for outer lane pedestrians. The steep gradient stems from the unevenness of the distribution of pedestrians; however, the increase in velocity of outer lane pedestrians is promoted by the space of the shorter side of the corridor.

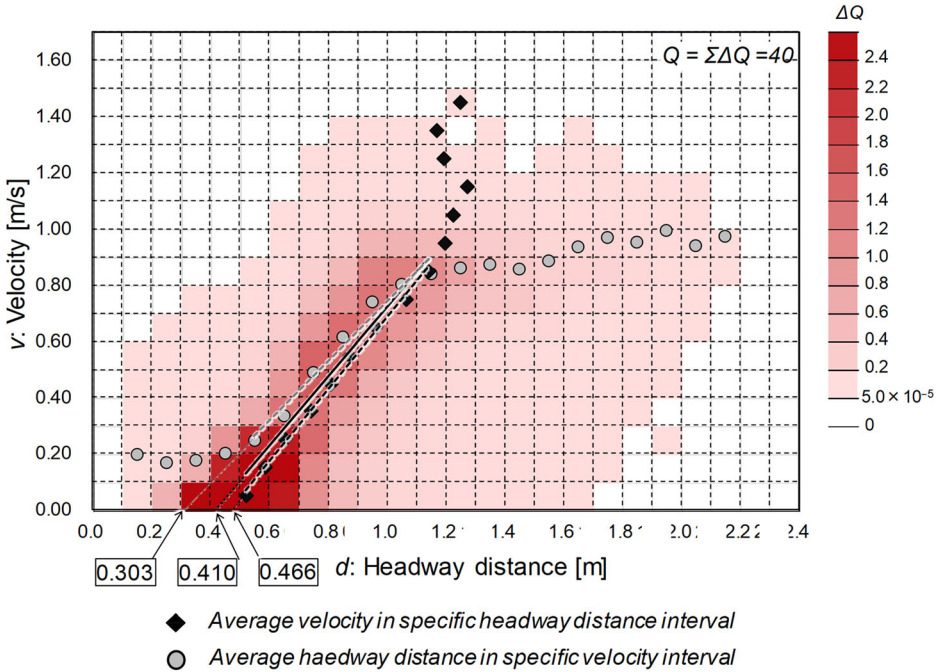
4.2.2. *Headway Distance-Velocity Distribution* Figures 7, 8, 9, 10 and 11 (right) show the normalized headway distance-velocity distributions. In these graphs, the headway distance and velocity of the two trials are plotted in the 0.01 m and 0.01 m/s intervals from normalization by formulas (1) and (2). As an exception, the interval from 0 m/s to 0.01 m/s includes the negative velocity data acquired from the wobbling of stopped pedestrians. In Case 1, the mode headway distance



was 0.98 m, the mode velocity was 0.82 m/s, and approximately 65% of the headway distance was within 0.8 m to 1.2 m. In contrast, the percentage of large headway distance was high; approximately 25% of the headway distance was greater than 1.2 m, and in this range, the velocity was mainly distributed within 0.8 m/s to 1.0 m/s. This distribution means that the pedestrians maintained the same velocity as the surrounding pedestrians. In Case 2, the mode headway distance was 0.76 m, the mode velocity was 0.54 m/s, and the distribution range of the headway distance was smaller than that of Case 1. Compared with Case 2, the percentage of large headway distances greater than 1.2 m is small, approximately 6.3%. In Case 3, the average headway distance was 0.6 m, and the average velocity was 0.2 m/s. Comparing Case 1 and Case 2, the shape of the velocity distribution, which can be regarded as a normal distribution, is almost the same; however, the absolute values are different. Focusing on Case 3, which is similar to the shape of the distribution of Case 1 and Case 2, the smaller side of the distribution reaches zero velocity, and the percentage of velocity smaller than 0.01 m/s becomes large, at approximately 3%. Thus, the shape of the velocity distribution is similar, and absolute values differ between “Case 1 and Case 2”; “Case 3” means that the relative difference in velocity within Case 3 is larger than that of Case 1 and Case 2, and this relative difference in velocity causes unstable homogeneous flow and multiple gradients in the time–space diagram. In Case 4 and Case 5, the percentage of  $v = 0$  m/s was high. This is thought to have caused stop-and-go behavior. As discussed in Sect. 4.2.3, the headway distance range where pedestrians were almost stopped was 0.4 m to 0.5 m. Figures 10 and 11 show that the headway distance of more than half of the pedestrians was less than 0.5 m. This headway distribution presumably generated stop-and-go behavior. Figures 7, 8 and 9 show that in Case 1 and Case 2, there were few pedestrians with headway distances less than 0.5 m, which can explain why stop-and-go behavior did not occur. In contrast, in Case 3, the percentage of pedestrians with a headway distance less than 0.4 m was 7%, and that of 0.5 m was 22%. This is assumed to have generated unevenness in the velocity as the seed of stop-and-go walking.

*4.2.3. Relationship Between the Headway Distance and Velocity* Figure 12 shows the consolidated normalized  $d$ - $v$  plots of all experimental cases acquired by formulas (3) and (4). The  $d$ - $v$  plots are widely distributed. This distribution means that a specific headway distance did not always yield a unique velocity. However, the peak of the distribution was almost linear in the range of  $0.55 \leq d \leq 1.15$ .

Figure 12 shows two kinds of average values. One is the average velocity in the interval of headway distance, and the other is the average headway distance in the interval of velocity. These average values coincided with the distribution peak in the range of  $0.55 \leq d \leq 1.15$  and  $0.05 \leq v \leq 0.85$  in a linear relationship. This relationship means that headway distance and velocity were uniquely specified. In contrast, the average velocities in the headway distance range larger than 1.15 m were almost constant (approximately 0.9 m/s). The average headway distance in the velocity range larger than 0.85 m/s was also almost constant (approximately 1.2 m). This means that the pedestrians were walking at their desired velocity and headway distance in those ranges. In addition, the average velocities in the head-



Regression formulas

- ◆---  $v = 1.28d - 0.600 = 1.28(d - 0.466), (0.05 \leq v \leq 0.85), R^2 = 0.9959$
- $v = 1.06d - 0.322 = 1.06(d - 0.303), (0.55 \leq d \leq 1.15), R^2 = 0.9721$
- ◆—○—  $v = 1.20d - 0.494 = 1.20(d - 0.410), (0.52 \leq d \leq 1.15), R^2 = 0.9431$

**Figure 12. Headway distance-velocity distribution of all experimental data.**

way distance range smaller than 0.55 m were almost constant (approximately 0.2 m/s). This velocity is assumed to be the minimum velocity of pedestrians walking. From the video, the pedestrians in this situation do not walk by moving their legs rhythmically, which was described by Kitagawa [46] and Thompson [47] as a “step cycle”, but they walk foot by foot. This velocity is thought to be governed by the minimum one-step velocity and minimum one-step gait.

In the range of  $0.05 \leq v \leq 0.85$ , the following regression formula can be acquired from the average velocity in a specific headway distance interval with  $R^2 = 0.9959$ :

$$v = 1.28d - 0.600 = 1.28(d - 0.466), \quad (0.05 \leq v \leq 0.85) \tag{5}$$

In the range of  $0.55 \leq d \leq 1.15$ , the following regression formula can be acquired from the average specific headway distance in the velocity interval with  $R^2 = 0.9721$ :

$$v = 1.06d - 0.322 = 1.06(d - 0.303), \quad (0.55 \leq d \leq 1.15) \tag{6}$$

In the range of  $0.05 \leq v \leq 0.85$  and  $0.55 \leq d \leq 1.15$ , the following regression formula can be acquired from two kinds of average values with  $R^2 = 0.9431$ :

$$v = 1.20d - 0.494 = 1.20(d - v0.410), \quad (0.52 \leq d \leq 1.15) \tag{7}$$

Figure 12 also shows these graphs. Suppose that the headway distance is uniquely decided by the velocity. The  $x$ -intercept of formula (5) of 0.466 m can be regarded as the ideal minimum headway distance because  $v = 0$  m/s at this headway distance. The gradient of formula (6) is smaller than those of formulas (5) and (7). However, for example, if the regression formulas were acquired in the range of  $0.65 \leq d \leq 1.15$ , the gradients of all formulas become almost the same. This means that dispersion at small headway distances ( $d \leq 0.65$ ) and low velocities ( $v \leq 0.20$ ) is relatively large.

Suppose that the headway distance and velocity uniquely correspond with each other and that their relationship is formula (7). The distribution of pedestrians is homogeneous, and the flow rate  $F$  (people/s) is described as follows:

$$F = v/d = 1.20(1 - 0.410/d) \quad (0.55 \leq d \leq 1.15) \tag{8}$$

This formula means that the flow rate is inversely proportional to the headway distance between pedestrians. The constant term of formula (8) of 1.20 people/s can be regarded as the ideal maximum flow rate because the flow rate converges to the increase in headway distance, even though the range of  $d > 1.15$  m is out of the valid range acquired from the experiment. Using linear density  $\rho_1 = 1/d$  (people/m), this formula can be expressed as follows:

$$F = -0.410\rho_1 + 1.20 \quad (0.870 \leq \rho_1 \leq 1.82) \tag{9}$$

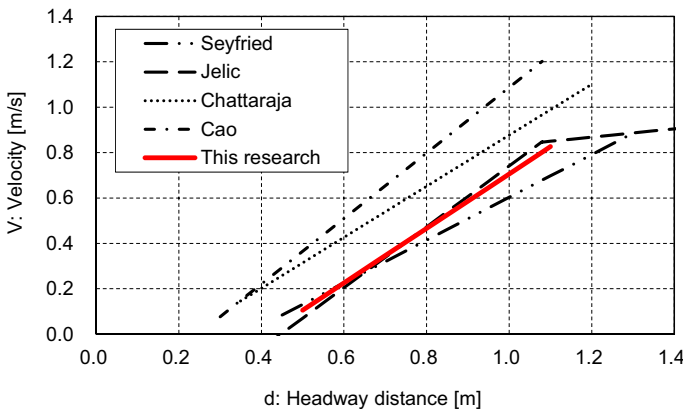


**Figure 13. Comparison with previous experiments of the headway distance to velocity.**

**Table 2**  
**Settings of Previous Experiments and Our Experiment**

Data source	Seyfried [24]	Jelic [29]	Chattaraja [35]	Cao [31]	This research
Nationality	Germany	France	India	China	Japan
Test participants	Age Gender	a) Male and female	a) Male only	– –	20–25 Male and female
Instruction	–	Walk in natural way	–	Walk in normal way	Evacuation. Do not run but swiftly
Definition of headway distance	–	Between the center of body mass	–	Between the center of heads	Between the center of heads
Path geometry	0.8 m Single-file	Ring corridor <sup>b)</sup> /Walk along with the inner or outer walls in a single line	0.8 m Single-file	0.8 m Single-file	1.2 m corridor/ Naturally formed two lanes
Path construction	Pipe chairs	Walls with the high of test participants	Pipe chairs	Walls with the high of test participants	1.8 m high walls
Note	c)	–	c)	d)	d)

a) Age of the test participants has not been dictated in the main text; however, those papers show the pictures of the experiments, and the test participants shown there seems to be 20–40's in Seyfried [24] and Jelic [29] experiments, and 20–30's in Chattaraja [35] experiment. Seyfried [24] mention that the test participants are consisted of the student and staff and Chattaraja [35] mention that the test participants are only students

b) Formed by inner and outer circular walls of radii 2 and 4.5 m, respectively

c) Test participants held number cards in their hand

d) Test participants wore colored caps for image processing

This formula means that the flow rate linearly decreases with an increase in the linear density.

*4.2.4. Comparison with Previous Experiments* Figure 13 and Table 2 show the comparison with previous single-file experiments [24, 29, 31, 35] (Cao [31] also showed the same comparison). Our result is similar to Jelic's [29] result. This means that the gradient of the headway distance to velocity is approximate the same as Cao [31] and Jelic's [29] results. In contrast, the gradients of Seyfried [24] and Chattaraja [35] are approximate and smaller than those of Cao [31], Jelic [29], and our results. The reason for this difference is not clear. However, we can speculate on some aspects. For example, compared with the experimental settings, Seyfried [24] and Chattaraja [35] composed their corridor by pipe chairs with test participants waist high and test participants holding number cards. In contrast, Cao [31] and Jelic [29] constructed experimental corridors with walls of almost the

same height as the test participants, and test participants had nothing in their hands while walking. Suppose the  $d$ -axis intercept is an imaginary minimum distance for pedestrians to stop, the minimum value is 0.25 m for Cao’s data [31] and the maximum value is 0.44 m for Jelic’s data [29]. Our value is 0.41 m, which is a relatively large value. The reason for this distribution is also not clear; however, cultural background to accept a smaller headway distance, the composition of gender mixtures, or instruction may influence their behavior. For our experiment, some test participants tended to come alongside adjoining test participants or avoid coming alongside. Overall, the  $d$ - $v$  relationship of our experiment, which had a realistic corridor width, is within the range of previous single-file investigations.

### 4.3. Macroscopic Analysis: Relationships Between the Density, Velocity and Flow Rate

4.3.1. *Limitations* In this analysis, we acquired the velocity, specific flow and density of the experiments as the time-average value from 10 to 60 s after the walking starts. Note that if the pedestrians have homogeneous and constant densities, the time-average density would be 1.28, 1.71, 2.35, 2.78, or 3.42 people/m<sup>2</sup>; however, there are some deviations in the high-density range, especially in the high-density cases. This deviation is thought to come from the unevenness of pedestrian allocation, even though we tried to allocate them as uniformly as possible.

Consider the difference between the density of this experiment and that of the actual pedestrian. In this experiment, most pedestrians walked in the center of one of two lanes formed in a 1.2 m width corridor. Therefore, they walked in lanes 0.6 m wide in every density case and only differed in headway distance. In contrast, actual pedestrians (not in the experimental situation) change their distance

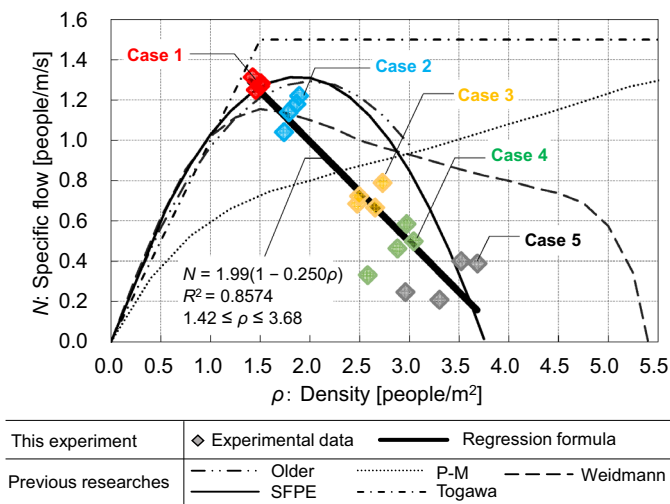


**Figure 14. Relationship between the density and specific flow.**

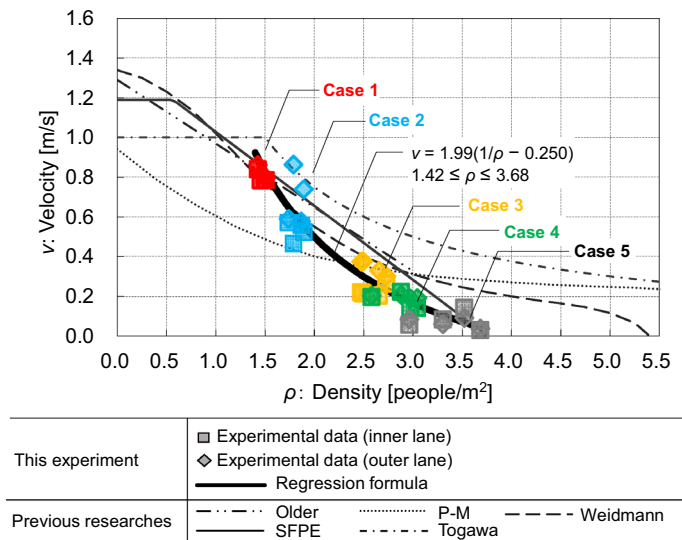


**Figure 15. Relationship between the density and velocity.**

to neighboring pedestrians or walls according to the density. Assuming the same high-density situation between actual pedestrians and experimental pedestrians, there is a possibility that actual pedestrians have smaller lateral distances and larger headway distances compared with experimental pedestrians because the corridor width basically fixes the lateral distance in this experiment. Therefore, if the relationship of formula (7) is applicable, the velocity of this experiment was lower than that of actual pedestrians. In contrast, the width distance of this experiment is thought to be greater than that of actual pedestrians, which might have caused the velocity in this experiment to be higher than that of usual pedestrians. Therefore, this comparison has to be interpreted with the consideration of these differences.

4.3.2. Results Figure 14 shows the data plots of density with respect to specific flow from this experiment and the regression formula acquired by the least mean square approximation. In addition, the preceding fundamental diagrams of Older [12], Predtechenskii-Milinskii [13] (P-M), Weidmann [14], SPFE [16], and Togawa [18] are presented in this graph. Figure 15 shows the data plots of density with respect to velocity and the preceding fundamental diagrams. The regression formula is also presented in Fig. 15. In Fig. 15, we distinguish the velocity data of the inner lane pedestrians and outer lane pedestrians. The velocity of the outer lane of Case 2 was slightly larger than that of the inner lane; however, there were few differences between the inner and outer lanes.

The relationship between the density and velocity seems to be approximately linear; however, considering that the microscopic analysis showed that the specific flow increased linearly with the density, we applied a linear regression formula to

the relationship between density and specific flow. In Fig. 14, the regression formula between density and specific flow is as follows, with  $R^2 = 0.8574$ .

$$N = 1.99 (1 - 0.250\rho)(1.42 \leq \rho \leq 3.68)(10).$$

For reference, suppose the imaginary linear density  $\rho_1'$  (people/m) can be defined by  $\rho$  and 0.6 m lane width as  $\rho_1' = 0.6\rho$ . Formula (10) is translated into imaginary flow rate  $F'$  (people/s) as follows:

$$F' = 0.6 N = -0.498\rho_1' + 1.19(0.852 \leq \rho_1' \leq 2.21) (11).$$

Comparing formulas (9) and (11), even though the coefficients of  $\rho_1$  and  $\rho_1'$  differ by approximately 20%, the formulas are similar. The difference in the coefficient is thought to be due to the dispersion of specific flows of Case 4 and Case 5 in Fig. 14. Therefore, formula (10) is essentially convertible to formula (9) as long as the width of the corridor or lanes does not affect the flow. However, the modeling of the fundamental diagram from the headway distance and velocity is relatively accurate, and modeling from the density to flow rate tends to involve error by dispersion or uncertainty.

In Fig. 14, there are two data plots with relatively large deviations from this regression formula: 2.6 people/m<sup>2</sup> in Case 4 and 2.9 people/m<sup>2</sup> in Case 5. From the video record, crowd flow was essentially very scarce. Some pedestrians in relatively low-density areas hardly moved even though they had relatively large headway distances compared to the other pedestrians because the pedestrian in front did not move. Therefore, the density of these areas was relatively low compared to their average specific flow.

The regression formula between density and velocity shown in Fig. 15 was calculated from the above formula considering the relationship  $v = N/\rho$ ; this means that it was not acquired as the regression of the plot of the density with specific flow in Fig. 15.

$$v = 1.99 (1/\rho - 0.250)(1.42 \leq \rho \leq 3.68)(12).$$

This formula also approximated the experimental plots well.

**4.3.3. Discussion** The density range obtained in this experiment corresponds to a density higher than that of “free walking” in the studies by Older [12], Togawa [18], and SFPE [16]. In the free walking situation, the velocity is almost constant or exhibits small changes with changes in the density, and the specific flow increases almost proportionally to the density. The relationships between the density and velocity and density and specific flow obtained in this experiment match Older’s [12] and SFPE’s [16] formulas as representatives of the regression formula types, even though the velocity and specific flow are slightly lower. However, for the other formulas, the following aspects are very different. In P-M’s formula [13], the specific flow increases with increasing density. In Togawa’s formula [18], the specific flow is constant at a high density. In Weidmann’s formula [14], the specific flow decreases with increasing density, and the decrease in specific flow is relatively small.

The style of the regression formulas of this experiment in which the velocity decreases inversely and the specific flow decreases linearly with increasing density is different from those of the preceding regression formulas, such as the SFPE model [16], which is based on the concept of Fruin [21] and Paul [22]. This differ-



ence might stem from what kind of formula is used for the regression. However, this difference is thought to suggest the following. The formula of the specific flow of the SFPE model [16] shows a convex curve with its peak in the positive direction, and the density that gives the largest specific flow is 1.88 people/m<sup>2</sup>. In contrast, this experiment's maximum specific flow is given at the lowest density of 1.42 people/m<sup>2</sup> within the applicability limit. The parameter of 1.42 people/m<sup>2</sup> is set due to the experimental setting of the minimum density. However, considering Fig. 7, the velocity at a large headway distance (low density) condition was almost the same at 0.9 m/s. If the velocity of low density is constant at 0.9 m/s, the specific flow of this density range becomes a linear function; therefore, this marginal density of linear  $d$ - $N$  pedestrian flow is thought to give the maximum specific flow. However, lower-density data are needed to discuss the possibility of the maximum specific flow.

In contrast, the density that gives the maximum specific flow in SFPE's formula [16] is given only half the value of the maximum density. SFPE's formula is simple and easy to use because the whole density range of velocity/specific flow is expressed by one formula. However, this experiment's regression formula suggests that the maximum specific flow is acquired as the marginal density of linear  $d$ - $N$  pedestrian flow under high-density conditions or the marginal density of constant velocity under low-density conditions. In addition, the maximum specific flow density is lower than half of the density, which gives zero velocity.

## 5. Conclusions

To understand the evacuation behavior in corridors or circulation space connected to the fire rooms and stairs, the relationships between the headway distance, density, velocity, and specific flow were examined using loop corridor experiments. The following findings were acquired.

1. The relationship plot between the headway distance  $d$  (m) and velocity  $v$  (m/s) is widely distributed. However, for  $0.55 \leq d \leq 1.15$ ,  $v$  increases linearly with increasing  $d$ . This relationship means that the specific flow  $N$  (people/m/s) decreases linearly with increasing linear density  $\rho_l$  (people/m) in the range  $0.870 \leq \rho_l \leq 1.82$ . This linear  $d$ - $v$  relationship is similar to the results of previous single-file experiments [24, 29, 31, 35]; therefore, confined corridor crowd flow can be discussed focusing on the headway distance and velocity relationship.
2. In the above situation, the ideal minimum headway distance in the linear relationship is approximately 0.4–0.5 m. Especially from the extrapolation of the above regression, this value is 0.466 m. Under smaller headway distance conditions, the average pedestrian velocity becomes approximately 0.2 m/s.
3. In the experimental case crowd, the density ranges from 1.42 people/m<sup>2</sup> to 1.71 people/m<sup>2</sup>, and the pedestrian flow is almost homogeneous in density, velocity, and specific flow. However, in the cases where the crowd density is over 2.35 persons/m<sup>2</sup>, pedestrians cannot walk at constant speed and exhibit stop-and-go

behavior. In this case, longitudinal waves of low-density areas are generated. This behavior occurs because the percentage of pedestrians whose headway distance is smaller than the ideal minimum headway distance increases.

4. The density to specific flow is acquired as a linear function. The maximum specific flow is acquired at the marginal minimum density where a linear relationship is maintained. In addition, the maximum specific flow is given at densities lower than half of the maximum density, which gives zero velocity. Compared with popular fundamental diagrams such as SFPE's formula [16], the average specific flow is a quadratic function of the density, and the maximum specific flow is given in half the density of the maximum value. This modeling represents the different facets of low-density pedestrian flow and high-density pedestrian flow well.

In the lowest density case of  $1.42 \text{ people/m}^2$  (Case 1), most of the velocity distribution is  $0.9 \text{ m/s}$ , and this velocity is thought to be the free walking velocity. However, this research does not cover lower density cases, which can be thought of as free walking velocity situations. In addition, the path width is fixed as  $1.2 \text{ m}$  which allow the pedestrians to form two lanes naturally. This path width setting is more realistic than single-lanes experiments [24, 28–36] which concern relationship between the headway distance and velocity. However, the bottleneck flow experiments [1–11] show the effect of the bottleneck width for specific flow and the density in front of the bottleneck. We would like to plan a further research about low-density flow situations and effect of path width in the future.

In high-density situations, especially in stop-and-go behavior situations, we observe pedestrian walking behavior from videos in which pedestrians do not walk by moving their legs rhythmically but walk foot by foot. In addition, we note the possibility that the velocity is governed by the minimum one-step velocity and minimum one-step gait. This suggests that the mechanism of walking behavior might be different for different density or headway distance situations. Analysis and modeling of these differences will be included in our future research.

## Funding

This research was funded by the “Collaborative Use and Research Fund of the Research Center for Fire Safety Science,” Tokyo University of Science, 2015. The experiments were conducted by the joint research group of the Akeno Facility Resilience Institute, FDM, Obayashi Corporation, Kajima Corporation, Shibaura Institute of Technology, Shimz Corporation, National Research Institute for Fire and Disaster, Taisei Corporation, Takenaka Corporation, Tokyo University of Science, and Waseda University (all are in Japan, in Japanese alphabetical order). We would like to express our gratitude to all those who have supported our research.

## Code Availability

Not applicable.

## Declarations

**Conflict of interest** The authors declare that there are no conflicts of interest.

**Ethical approval** This experiment was approved by the Research Ethics Committee at Waseda University as part of the research program entitled “Empirical study about the effects of obstacles on pedestrian crowd dynamics.”

## References

1. Seyfried A, Steffen B, Winkens A, Rupperecht T, Boltes M, Klingsch W (2007) Empirical data for pedestrian flow through bottlenecks. *Traffic Granular Flow* 07:189–199. [https://doi.org/10.1007/978-3-540-77074-9\\_17](https://doi.org/10.1007/978-3-540-77074-9_17)
2. Steffen B, Seyfried A (2010) Methods for measuring pedestrian density, flow, speed and direction with minimal scatter. *Physica A* 389:1902–1910. <https://doi.org/10.1016/j.physa.2009.12.015>
3. Daamen W, Hoogendoorn SP (2012) Emergency door capacity: Influence of door width, population composition and stress level. *Fire Technol* 48:55–71. <https://doi.org/10.1007/s10694-010-0202-9>
4. Zhang J, Seyfried A (2014) Quantification of bottleneck effects for different types of facilities. *Transp Res Proc* 2:51–59. <https://doi.org/10.1016/j.trpro.2014.09.008>
5. Yang H, Cheng X, Zhang H, Yang H, Yuen RKK (2014) Effect of right-hand traffic rules on evacuation through multiple parallel bottlenecks. *Fire Technol* 50:297–316. <https://doi.org/10.1007/s10694-013-0370-5>
6. Fujii K, Yamaguchi J, Ohmiya Y, Tange M, Jo A, Sano T (2017) Effect of opening width on pedestrian flow during passing through an opening in wide space—Pedestrian characteristics of crowd evacuation in space of various shapes. *J Architect Plann AIJ* 82(733):601–611. <https://doi.org/10.3130/aija.82.601>
7. Shi X, Ye Z, Shiwakoti N, Tang D, Lin J (2019) Examining effect of architectural adjustment on pedestrian crowd flow at bottleneck. *Physica A* 522:350–364. <https://doi.org/10.1016/j.physa.2019.01.086>
8. Li H, Zhang J, Yang L, Song W, Yuen KKR (2020) A comparative study on the bottleneck flow between preschool children and adults under different movement motivations. *Saf Sci* 121:30–41. <https://doi.org/10.1016/j.ssci.2019.09.002>
9. Li H, Zhang J, Song W, Yuen KKR (2021) A comparative study on the bottleneck flow under different movement motivations. *Fire Saf J* 120:103014. <https://doi.org/10.1016/j.firesaf.2020.103014>
10. Imanishi M, Jo A, Sano T (2021) Effects of pedestrian motivation and opening shape on pedestrian flow rate at an opening. *Fire Saf J* 120:103056. <https://doi.org/10.1016/j.firesaf.2020.103056>

11. Georg P, Schumann J, Holl S, Boltes M, Hofmann A (2021) The influence of individual impairments in crowd dynamics. *Fire Mater* 45:529–542. <https://doi.org/10.1002/fam.2789>
12. Older SJ (1968) Movement of Pedestrians on footways in shopping streets. *Traffic Eng Control* 10:160–163
13. Predtechenskii VM, Milinskii AI (1978) Planning for foot traffic flow in buildings. Amerind, New Delhi
14. Weidmann U (1993) Transporttechnik der Fussgänger. Schriftenreihe des IVT 90, ETH Zürich. <https://doi.org/10.3929/ethz-a-000687810>
15. Helbing D, Johansson A, Al-Abideen HZ (2007) Dynamics of crowd disasters: An empirical study. *Phys Rev E* 75:046109. <https://doi.org/10.1103/PhysRevE.75.046109>
16. Gwynne SMV, Rosenbaum RR (2008) Employing the hydraulic model in assessing emergency movement. The SFPE handbook of fire protection engineering fourth edition, SFPE/NFPA 3-373-3-396
17. Kimura K, Ihara S (1937) A survey for the state of crowds streaming in building. *J Architect Plann Environ Eng* 5:307–316(in Japanese)
18. Togawa K (1963) Study on fire escape basing on the observation of multitude currents. Doctoral thesis, The University of Tokyo (in Japanese)
19. Mori M, Tsukaguchi H (1977) Pedestrian movements on footways. *J Jpn Soc Civil Eng* 268:99–108(in Japanese)
20. Jin T (1983) Variation of the crowd and its walking speed. *J Jpn Assoc Fire Sci Eng* 33:8–12(in Japanese)
21. Fruin JJ (1971) Pedestrian planning design. Metropolitan Association of Urban Designers and Environmental Planners Inc, New York
22. Pauls JL (1980) Effective-width model for evacuation flow in buildings. In: Proceedings, engineering applications workshop, Society of Fire Protection Engineers, Boston
23. Daamen W, Hoogendoorn SP (2003) Experimental research of pedestrian walking behavior. *Transp Res Board Annu Meet* . <https://doi.org/10.3141/1828-03>
24. Seyfried A, Steffen B, Klingsch W, Boltes M (2005) The fundamental diagram of pedestrian movement revisited. *J Stat Mech: Theory Exp* 10:10002–10002. <https://doi.org/10.1088/1742-5468/2005/10/p10002>
25. Seyfried A, Steffen B, Lippert T (2006) Basic of modelling the pedestrian flow. *Physica A* 368:232–238. <https://doi.org/10.1016/j.physa.2005.11.052>
26. Seyfried A, Boltes M, Kähler J, Klingsch W, Portz A, Rupprecht T, Schadschneider A, Steffen B, Winkens A (2008) Enhanced empirical data for the fundamental diagram and the flow through bottlenecks. *Pedestr Evacuation Dyn* . [https://doi.org/10.1007/978-3-642-04504-2\\_11](https://doi.org/10.1007/978-3-642-04504-2_11)
27. Minegishi Y, Takeichi N (2018) Design guidelines for crowd evacuation in a stadium for controlling evacuee accumulation and sequencing. *Jpn Archit Rev* 1(4):471–485. <https://doi.org/10.1002/2475-8876.12042>
28. Portz A, Seyfried A (2011) Analyzing stop-and-go waves by experiment and modeling. *Pedestr Evacuation Dyn* . [https://doi.org/10.1007/978-1-4419-9725-8\\_52](https://doi.org/10.1007/978-1-4419-9725-8_52)
29. Jelic A, Cecile AR, Lemercier S, Pettre J (2012) Properties of pedestrians walking in line: fundamental diagram. *Phys Rev E* 85:036111. <https://doi.org/10.1103/PhysRevE.85.036111>
30. Fang Z, Song W, Liu X, Lv W, Ma J, Xiao X (2012) A continuous distance model (CDM) for the single-file pedestrian movement considering step frequency and length. *Physica A* 391:307–316. <https://doi.org/10.1016/j.physa.2011.08.009>
31. Cao S, Zhang J, Salden D, Ma J, Shi C, Zhang R (2016) Pedestrian dynamics in single-file movement of crowd with different age compositions. *Phys Rev E* 94:012312. <https://doi.org/10.1103/PhysRevE.94.012312>

32. Jin C, Jiang R, Li R, Li D (2019) Single-file pedestrian flow experiments under high density conditions. *Physica A* 531:121718. <https://doi.org/10.1016/j.physa.2019.121718>
33. Cao S, Wang P, Yao M, Song W (2019) Dynamic analysis of pedestrian movement in single-file experiment under limited visibility. *Commun Nonlinear Sci Numer Simul* 69:329–342. <https://doi.org/10.1016/j.cnsns.2018.10.007>
34. Cao S, Chen M, Xu L, Liang J, Yao M, Wang P (2020) Analysis of headway velocity relation in one and two-dimensional pedestrian flows. *Saf Sci* 129:104804. <https://doi.org/10.1016/j.ssci.2020.104804>
35. Chattaraj U, Seyfried A, Chakroborty P (2009) Comparison of pedestrian fundamental diagram across cultures. *Adv Complex Syst* 12(3):393–405. <https://doi.org/10.1142/S0219525909002209>
36. Ma Y, Lee EWM, Shi M, Yuen RKK (2021) Spontaneous synchronization of motion in pedestrian crowds of different densities. *Nat Hum Behav* 5:447–457. <https://doi.org/10.1038/s41562-020-00997-3>
37. Bolts M, Seyfried A, Steffan B, Schadschneider A (2008) Automatic extraction of pedestrian trajectories from video recordings. *Peestr Evacuation Dyn* 2008:43–54. [https://doi.org/10.1007/978-3-642-04504-2\\_3](https://doi.org/10.1007/978-3-642-04504-2_3)
38. Liu X, Song W, Zhang J (2009) Extraction and quantitative analysis of microscopic evacuation characteristics based on digital image processing. *Physica A* 338:2717–2726. <https://doi.org/10.1016/j.physa.2009.03.017>
39. Tian W, Song W, Ma J, Fang Z, Seyfried A, Liddle J (2012) Experimental study of pedestrian behaviors in a corridor based on digital image processing. *Fire Saf J* 47:8–15. <https://doi.org/10.1016/j.firesaf.2011.09.005>
40. Tange M, Imanishi M, Sano T, Ohmiya Y (2016) Image processing of pedestrian behavior with multiple color markers and its application to crowd evacuation experiment. *Journal of architecture and planning, Architectural Institute of Japan* 81(730):2645–2652. [https://doi.org/10.3130/aija.81.2645in Japanese](https://doi.org/10.3130/aija.81.2645in%20Japanese)
41. NFPA 101 Life Safety Code (2021), Chapter 12, 12.2.3.8 Minimum corridor width
42. Order for Enforcement of the Building Standard Law of Japan (2021), Article 119 Corridor width **(in Japanese)**
43. Ren X, Zhang J, Song W, Cao S (2019) The fundamental diagrams of elderly pedestrian flow in straight corridors under different densities. *J Stat Mech* 2019:023403. <https://doi.org/10.1088/1742-5468/aafa7b>
44. Furukawa Y, Tsuchiya S, Inahara S, Hasemi Y (2004) Reproducibility of the group evacuation behavior of the elderly by subjects wearing elderly simulator. *J Environ Eng* 69(581):9–14. [https://doi.org/10.3130/aije.69.9\\_5in Japanese](https://doi.org/10.3130/aije.69.9_5in%20Japanese)
45. Minegishi Y (2021) Experimental study of the walking behavior of crowds mixed with slow-speed pedestrians as an introductory study of elderly-mixed evacuation crowds. *Fire Saf J* 120:103041. <https://doi.org/10.1016/j.firesaf.2020.103041>
46. Kitagawa A, Ogihara N (2016) Estimation of foot trajectory during human walking by a wearable inertial measurement unit mounted to the foot. *Gait Posture* 45:110–114. <https://doi.org/10.1016/j.gaitpost.2016.01.014>
47. Thompson P, Nilsson D, Boyce K, Molloy M, McGrath D (2020) Exploring the biomechanics of walking and crowd “flow”. *Fire Mater* 44:879–893. <https://doi.org/10.1002/fam.2889>